

Nonparallel Stacks of Donor and Acceptor Chromophores Evade Geminate Charge Recombination

Ajith R. Mallia, P. S. Salini, and Mahesh Hariharan*

School of Chemistry, Indian Institute of Science Education and Research Thiruvananthapuram, CET Campus, Sreekaryam, Thiruvananthapuram, Kerala, India 695016

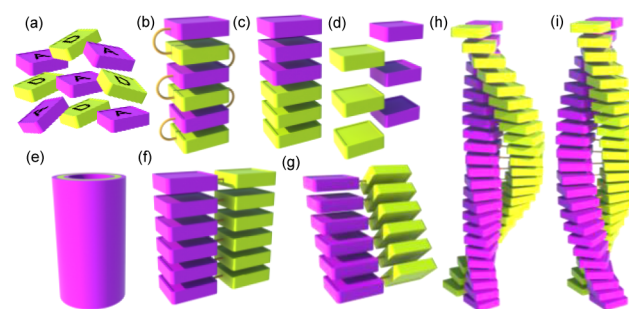
S Supporting Information

ABSTRACT: We report a nonparallel stacked arrangement of donor–acceptor (D–A) pairs for prolonging the lifetime of photoinduced charge-separated states. Hydrogen–hydrogen steric repulsion in naphthalimide–naphthalene (NIN) dyad destabilizes the planar geometry between the constituent units in solution/ground state. Sterically imposed nonplanar geometry of the dyad allows the access of nonparallel arrangement of the donor and acceptor stacks having triclinic space group in the crystalline state. Antiparallel trajectory of excitons in nonparallel D–A stacks can result in lower probability of geminate charge recombination, upon photoexcitation, thereby resulting in a long-lived charge-separated state. Upon photoexcitation of the NIN dyad, electron transfer from naphthalene to the singlet excited state of naphthalimide moiety results in radical ion pair intermediates that survive >10,000-fold longer in the aggregated state ($\tau_{cr}^a > 1.2$ ns) as compared to that of monomeric dyad ($\tau_{cr}^m < 110$ fs), monitored using femtosecond transient absorption spectroscopy.

Modulating the behavior of photogenerated excitons is crucial in the development of materials for artificial photosynthesis and photovoltaic device applications.¹ Precise spatial organization of electronically complementary chromophores is a prerequisite to afford long-lived photoinduced charge separation. Generation of photoinduced long-lived charge-separated states in isolated donor–acceptor (D–A) systems continues to possess enormous interest.² State-of-the-art theoretical³ and experimental⁴ investigations suggest that D–A systems that assemble to form extended architectures can effectively prolong the lifetimes of photogenerated excitons. Electron donors and acceptors tend to stack on one another by virtue of their electronic complementarity,⁵ thereby trapping and instantaneously annihilating the photogenerated charge carriers through geminate charge recombination.⁶ Attempts to circumvent the interdigitating arrangement of donor and acceptor include utilization of π – π stacking,⁷ hydrogen-bonded,⁸ cooperative,⁹ metal–ligand¹⁰ interactions, chiral auxiliaries,¹¹ and self-organizing surface-initiated polymerization.¹² Such approaches have provided defined oligomers to large aggregates possessing parallel,⁷ coaxial,⁶ contiguous,¹³ cylindrical,¹⁴ slipped,¹⁵ slipped-sandwich,¹⁶ double-helical,^{9,17} or helix wrapped columnar stacks¹⁸ of D–A chromophores (Scheme 1).

Our continued interest toward the design of near-orthogonally arranged D–A systems, for exploiting favorable photoprocesses

Scheme 1. Representative Strategies Adopted to Spatially Organize Electron Donors and Acceptors for Emergent Properties



in isolated¹⁹ and organized environment,²⁰ enabled us to restrict the cofacial arrangement²¹ of electronically complementary aromatic chromophores. A significant energy barrier (~ 100 kJ/mol)¹⁹ to rotation between naphthalene and naphthalimide units connected across single covalent bond enforces a nonplanar arrangement of the dyad in ACN solution. Spherical/ring-like architectures of the dyad formed in CHCl_3 , upon addition of hexane, crystallize as nonparallel stacks (Scheme 1g) of naphthalene and naphthalimide, in contrast to the disordered aggregates proposed for similar architectures.²² We herein report the first example of the formation of long-lived charge-separated states ($\tau_{cr}^a > 1.2$ ns) from the molecular aggregates of nonparallel arrangement of segregated D–A stacks upon photoexcitation.

Suzuki–Miyaura cross-coupling of 4-bromonaphthalimide with the corresponding arylboronic acids offered naphthalimide–naphthalene (NIN) and naphthalimide–phenyl (NIPh) dyads (Figure 1a, see Supporting Information, SI). In DCM:hexane (1:3) mixture, NIN and NIPh crystallize in triclinic (*P1*) and orthorhombic (*Pbcn*) space groups, respectively, whereas NI crystallizes in monoclinic (*P2₁/c*) space group (Table S1). The phenyl (Ph) and naphthyl (N) groups are tilted by 63° and 68° with respect to the NI plane in NIPh and NIN, respectively, suggesting nonparallel arrangement of constituents in the dyads (Figures 1 and S1). Quantum theory of atoms in molecules analysis (Figure S2) indicates strong dihydrogen interactions^{20,23} between (i) C–H moiety of NI and N units of adjacent dyad at a distance of 2.28 Å and (ii) the methylene protons of hydroxypropyl side-chain of two neighboring dyads at a distance of 2.27 Å. In addition, synergistic

Received: August 5, 2015

Published: October 6, 2015

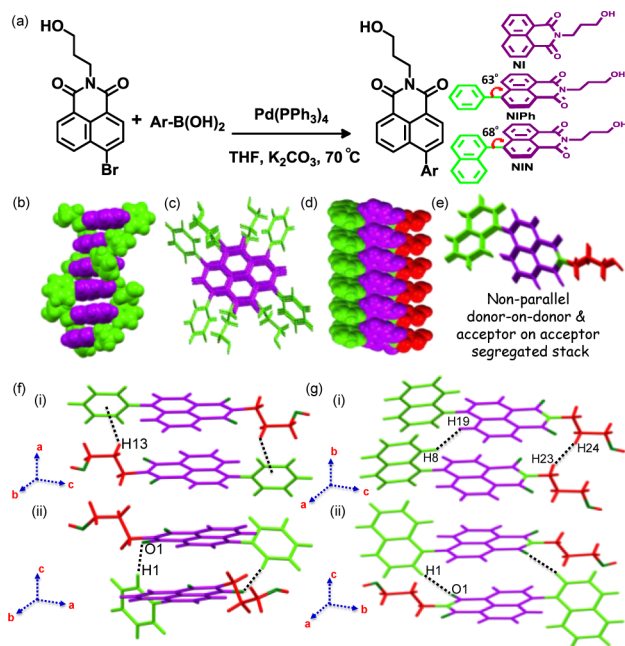


Figure 1. (a) Syntheses scheme for dyads NIPh and NIN with respective chemical structures. Packing arrangements of (b) NIPh (along “c” axis) and (d) NIN (along “b” axis). Perspective views of (c) NIPh and (e) NIN along “c” and “a” axes, respectively. Self-assembled structures of (f) NIPh and (g) NIN, respectively.

C–H $\cdots\pi$, π – π , and C–H \cdots O interactions along “b” axis further propagate nonparallel stacks resulting in donor-on-donor and acceptor-on-acceptor arrangement in crystalline NIN (Figure 1d,g-i). Nearest donor-to-donor and acceptor-to-acceptor π – π separations are found to be 3.76 and 3.55 Å, respectively. The intermolecular C–H \cdots O and C–H $\cdots\pi$ interactions along “a” axis constitute self-assembled structures in NIN (Figures 1g-ii and S3a,b) that do not have nonparallel donor and acceptor stacks. In NIPh, C–H $\cdots\pi$ interaction between methylene C–H of one molecule and the phenylic π -cloud of the adjacent one at a distance of 2.80 Å promotes the formation of an antiparallel stacked (3.60–3.89 Å; Figure 1f-i,ii) NIPh dimer. C–H \cdots O interaction between phenylic C–H and imidic oxygen at a distance of 2.62 Å and an angle of 170° connects two successive self-assembled dimers. The successive self-assembled dimers are rotated relative to each other by an angle of 65° resulting in a double helical organization with a pitch of 15.18 Å incorporating eight molecules per turn (Figure S3c).

Dynamic light scattering (DLS) experiments were performed to explore the existence and nature of NIN aggregates in solution (Figure 2a). DLS measurements of 0.1 mM NIN in CHCl₃ indicate the existence of aggregates with an average hydrodynamic diameter (D_H) of 350 nm. Successive increments (up to 2 mM) in concentration of NIN in CHCl₃ exhibit a bimodal distribution with D_H of 300 nm and 4.5 μ m. Nonequilibrium spherical aggregates that possess smaller D_H transform to larger aggregates with an increase in the concentration of NIN. Morphological analyses of 0.1 mM NIN in CHCl₃ using tapping mode AFM, SEM, TEM, and confocal microscopic techniques confirm the existence of spherical particles having an average size of 370–400 nm, which is in good agreement with the DLS measurement (Figures 2b,c and S4a–c).

At higher concentration (2 mM) of NIN in CHCl₃, spherical particles having an average diameter of 1.45, 1.67, and 1.86 μ m are observed from AFM, SEM, and confocal microscopic

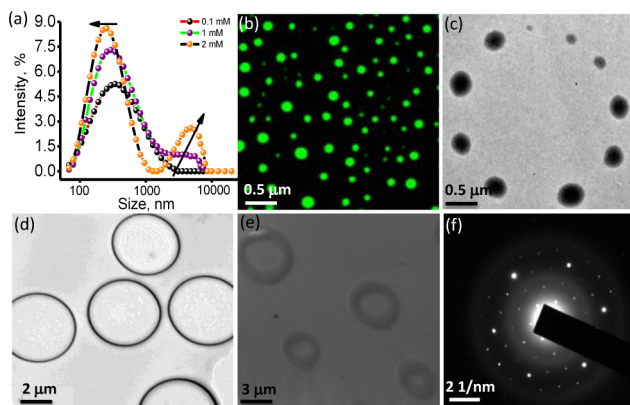


Figure 2. (a) Concentration-dependent particle size distribution of NIN from DLS; (b) confocal microscopic image of 2 mM NIN excited at 405 nm; TEM images of (c) 1 and (d) 2 mM NIN; (e) SEM image of NIN in CHCl₃ drop casted on carbon coated Cu substrate; (f) SAED pattern of NIN.

techniques (Figures S4d–f and S8). Co-existence of ring-like structures having an average diameter of 3.1 μ m along with the larger spherical particles is observed. Ring-like architectures further transform into discrete thick torroidal nanostructures (Figures 2d,e and S5–S8). Selected area electron diffraction (SAED) of NIN aggregates in CHCl₃ indicates single-crystalline nature having hexagonal/cubic crystal system (Figure 2f).²⁴ The amphiphilic nature of NIN enables the molecule to form bilayers in CHCl₃ at higher concentrations resulting in small spherical architectures that transform to larger spherical/ring-like architectures, consistent with similar amphiphilic molecules.²⁵ Such bilayer assembly could maintain the donor-on-donor and acceptor-on-acceptor arrangement even in the aggregated state similar to that observed in the crystalline state (Figure S8i,j, SI).

Having established the formation of nonparallel donor-on-donor and acceptor-on-acceptor stacks in the aggregated state, we have evaluated the ability of the system to prolong the long-lived charge-separated states. Frontier molecular orbital (FMO) analysis, UV–vis, fluorescence, and cyclic voltammetric measurements are employed to investigate the extent of perturbations in electronic interactions between donors (N/Ph) and acceptor (NI) in aggregated vs monomeric state of the dyads. FMO analyses of NIN and NIPh show that the electron density of HOMO is distributed in NI and N/Ph units, while electron density of LUMO is completely localized on NI unit. This is clearly suggestive of the presence of charge-transfer (CT) interaction between the constituents in the ground state (Figure S9 and Table S2), consistent with 4-substituted naphthalimide derivatives reported earlier.²⁶ A decrease in HOMO–LUMO gap (Figure S10) for the di/tetrameric vs monomeric NIN indicates the possibility of more favorable photoinduced charge separation in the aggregate when compared to the monomer.

UV–vis absorption spectra of NIN and NIPh in ACN exhibit bands centered around 270–280 and 350–353 nm, respectively, (Figure S11a,c,d). Both the short and long wavelength transitions are red-shifted (\sim 8–11 nm) compared to that of NI. The longer wavelength band in NIN and NIPh arises from a π – π^* (HOMO \rightarrow LUMO) transition that has CT character,²⁷ while the shorter wavelength band corresponds to a n – π^* (HOMO-1 \rightarrow LUMO) transition. Upon excitation at 340 nm, NIN and NIPh in ACN exhibit broad emission centered at 570 ($\tau_f = 4.15$ ns) and 430 ($\tau_f = 3.55$ ns) nm, respectively (Figure S11b,e,f). A significant red-shift (\sim 185 nm; Figure S11b) in the

emission maximum of NIN in ACN, compared to that of the NI, further confirms a very strong CT character in NIN. Solvent polarity established negligible changes in the absorption maxima and a substantial bathochromic shift of 125 and 27 nm, respectively, in the emission maxima (Figures S12a,b and S13a,b). With an increase in solvent polarity, a 49% enhancement in fluorescence quantum yield of NIPh is observed, which could be due to the decrease in the nonradiative rate constant (Figure S14a,b and Table S3). The difference between excited- and ground-state dipole moments in NIN and NIPh is estimated to be 8.02 and 4.17 D, respectively, employing Lippert–Mataga (L–M) equation (see SI). The degree of charge separation in NIN and NIPh is determined to be 38.61% and 21.10%, respectively, from the centers of the spin density distributions²⁸ and L–M plots (see SI). At higher concentrations (0.125 mM) of NIN in CHCl₃, a bathochromic shift of ~20 nm in UV–vis, emission, and excitation measurements suggests the possibility of aggregation in NIN (Figure S12d–f). Under similar conditions, NIPh in CHCl₃ exhibits no characteristic features corresponding to self-aggregation (Figure S13c,d). Spectroscopic features corresponding to aggregates of NIN are more prominent in the crystalline NIN, as expected (Figure S15).

A favorable ΔG_{ET} of -0.78 eV (see SI for Rehm–Weller analysis) for photoinduced electron transfer from N to singlet excited state of NI ($^1\text{NI}^*$) in NIN prompted us to employ femtosecond^{20a} and nanosecond transient absorption (fTA and nTA) techniques to investigate the existence of charge-transfer intermediates (CTIs) in the monomeric vs aggregated state of NIN. Upon excitation at 355 nm, nTA spectra of NIN in ACN/CHCl₃ exhibit absorption bands centered at 400 and 480 nm having a lifetime of 3.36 μs (Figure S16 and Table S4) that is characteristic of triplet absorption of NI ($^3\text{NI}^*$) chromophore.²⁹ The fTA measurement of NIN in ACN has positive absorption centered at 440 and 600 nm. NIN in ACN yielded single principal component having a lifetime of 1.99 ns, which could be attributed to the naphthalene T_1 ($\pi-\pi^*$) transition³⁰ (Figures 3a,c). Absence of CTIs in nTA/fTA measurements with significant population of triplet excited state of N/NI substantiates ultrafast charge separation^{9,15} followed by geminate charge recombination resulting in the formation of $^3\text{N}^*/^3\text{NI}^*$

(Figure S17), upon photoexcitation of NI, consistent with earlier reported similar D–A systems.^{19,28}

Upon excitation at 400 nm, fTA spectra of aggregated NIN in CHCl₃ exhibit positive absorption bands at 420, 550, 710, and 1020 nm (Figure 3b,d) that consist of four principal components obtained by global analyses and singular value decomposition (Figures 3d, S18, and 19c,d and Table S5). Right singular vector at 420 nm possessing a lifetime of 1.52 ns corresponds to the naphthalimide radical anion³¹ ($\text{NI}^{\bullet-}$), a twin absorption centered at 430 and 560 nm corresponds to naphthalene T_1 ($\pi-\pi^*$) transition³⁰ that decays with a lifetime of 2.02 ns (see SI), while the third right singular vector at 710 nm, having a lifetime of 2.53 ns, corresponds to naphthalene radical cation ($\text{N}^{\bullet+}$).³² We also observed a positive band centered at 1020 nm, a feature that is not found in the monomeric NIN, which undergoes time-dependent shift of ~60 nm. Positive band centered at 1020 nm having a lifetime >1.2 ns³³ corresponds to naphthalene dimer radical cation ($\text{N}_2^{\bullet+}$), as reported earlier.³² Observed time-dependent shift in the peak corresponding to $\text{N}_2^{\bullet+}$ could be attributed to the evolution of a radical cation with discrete $\pi-\pi$ stacks of naphthalene, as observed in $\pi-\pi$ stacks of peryleneimide.^{20a} In contrast, NIPh in ACN and CHCl₃ exhibits one principal component at 500 nm having a lifetime of 1.17 and 1.98 ns respectively, corresponding to $^1\text{NI}^*$ (Figures S18–20).²³

Cyclic voltammetry of (0.1 M *n*Bu₄NPF₆ in ACN) NIN and NIPh (Figure S21a and Table S2) exhibited oxidation peaks at 1.54 and 2.48 V, while reduction peaks appeared at -1.33 and -1.30 V respectively. Ph/N substitution at fourth position of NI induced significant perturbations in the oxidation potentials as compared to unsubstituted NI, while reduction potentials ($E_{\text{red}} = -1.33$ V vs SCE) exhibited negligible change as observed earlier.²⁷ At higher concentrations (15 mM, Figure S21b,c), reduction of NIN in CHCl₃ occurs 133 mV more positive compared to that at lower concentrations (1 mM). In contrast, NIPh under similar conditions (data not shown) exhibited concentration-independent redox behavior. Facile electrochemical reduction of aggregated NIN relative to monomer suggests alteration in thermodynamic feasibility for photoinduced charge separation/recombination in the monomeric vs aggregated NIN. Such perturbations in the redox properties are a direct consequence of delocalization of hole and electron in the NIN assembly consistent with the observation of $\text{N}_2^{\bullet+}$ using fTA spectroscopy.³⁴

In summary, a nonparallel segregated D–A stacked arrangement of a dyad formed by naphthalimide and naphthalene that undergo self-assembly in CHCl₃ by virtue of co-operative weak interactions is reported. The self-assembled D–A architecture thus generated can enhance the survival time of CTIs, upon photoexcitation, by $>10^4$ fold ($\tau_{\text{CT}}^{\text{a}}/\tau_{\text{CT}}^{\text{m}}$) in comparison to the monomeric NIN. Observed long-lived CTIs in the aggregated vs monomeric state of NIN possessing simple components could be corroborated to the synergistic effects induced by (i) nonplanar arrangement of the D–A pair and (ii) the delocalization of excitons across the nonparallel D–A stacks.

Significant smaller increases (Table S6) in the survival time of CTIs, ~1.5, 3, >100 and >150 -fold are observed in the aggregated state for cylindrical melamine-perylenediimide (PDI),¹⁴ chlorophyll-pyromellitimide-naphthalenediimide,³⁵ guanine-PDI G-quartet,^{10a} and diketopyrrolopyrrole (DPP)-PDI,⁹ respectively, in solution, relative to the respective monomeric dyads. In thin films, a 1000-fold enhancement in the survival time of CTIs was observed for DPP-PDI³⁶ when compared to the monomer. Solvent vapor annealed thin films of

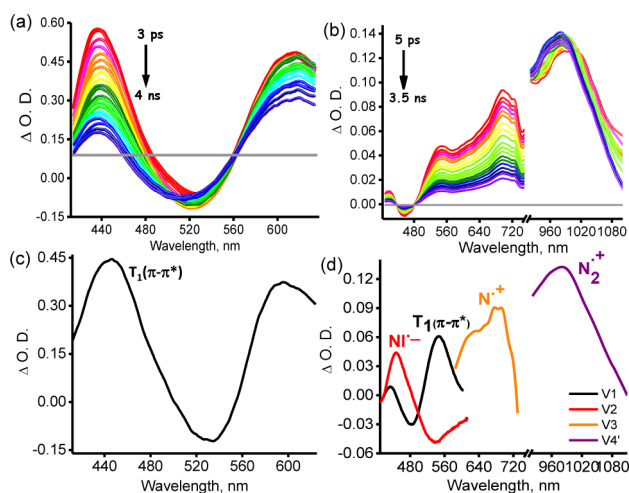


Figure 3. Femtosecond transient absorption spectra of 5 mM NIN in (a) ACN and (b) CHCl₃, (c and d) Right singular vectors obtained from singular value decomposition (see SI).

PDI-DPP-PDI¹⁵ reported by Wasielewski et al. yielded CTI lifetime of 4 μ s. Simple design and ease of processing exploiting synergistic effects offered by various nonbonded interactions make our strategy superior in moderating the behavior of CTIs in the aggregated state compared to the earlier “emergence-upon-assembly” approaches. Self-assembled nonparallel D–A architectures that possess a potential barrier for charge recombination with enhanced survival time of CTIs ($\tau_{cr}^a > 1.2$ ns)³³ could serve as promising scaffold for light harvesting, molecular electronics, and novel photofunctional applications.

■ ASSOCIATED CONTENT

Supporting Information

The Supporting Information is available free of charge on the ACS Publications website at DOI: 10.1021/jacs.5b08257.

Experimental methods and additional figures (PDF)

Crystallographic data (CIF)

Crystallographic data (CIF)

Crystallographic data (CIF)

■ AUTHOR INFORMATION

Corresponding Author

*mahesh@iisertvm.ac.in

Notes

The authors declare no competing financial interest.

■ ACKNOWLEDGMENTS

Authors thank Nanobiotechnology Task Force, DBT, Govt. of India for the support, BT/PR5761/NNT/106/599/2012; NIIST-TVM for TEM facility; A. P. Andrews for X-ray analysis; K. Nagarajan and Vinayak Bhat for computational support. Authors are grateful to Prof. F. D. Lewis and Dr. K. R. Gopidas for their valuable suggestions. The authors thank Mr. Shebin George for the cover artwork.

■ REFERENCES

- (1) Gélinas, S.; Rao, A.; Kumar, A.; Smith, S. L.; Chin, A. W.; Clark, J.; van der Poll, T. S.; Bazan, G. C.; Friend, R. H. *Science* **2014**, *343*, 512.
- (2) (a) Vura-Weis, J.; Abdelwahed, S. H.; Shukla, R.; Rathore, R.; Ratner, M. A.; Wasielewski, M. R. *Science* **2010**, *328*, 1547. (b) Zhang, Y.; Dood, J.; Beckstead, A. A.; Li, X.-B.; Nguyen, K. V.; Burrows, C. J.; Improta, R.; Kohler, B. *Proc. Natl. Acad. Sci. U. S. A.* **2014**, *111*, 11612. (c) Turro, N. J.; Ramamurthy, V.; Scaiano, J. C. Energy and Electron Transfer. In *Modern Molecular Photochemistry of Organic Molecules*, University Science Books: United States, 2010, pp 383. (d) For more references see SI.
- (3) (a) Difley, S.; Wang, L.-P.; Yeganeh, S.; Yost, S. R.; Voorhis, T. V. *Acc. Chem. Res.* **2010**, *43*, 995. (b) Lemaure, V.; Steel, M.; Beljonne, D.; Brédas, J.-L.; Cornil, J. *J. Am. Chem. Soc.* **2005**, *127*, 6077. (c) Savoie, B. M.; Jackson, N. E.; Chen, L. X.; Marks, T. J.; Ratner, M. A. *Acc. Chem. Res.* **2014**, *47*, 3385. (d) Siebbeles, L. D. A.; Grozema, F. C. *Charge and Exciton Transport through Molecular Wires*; Wiley-VCH: Germany, 2011.
- (4) (a) Gust, D.; Moore, T. A.; Moore, A. L. *Acc. Chem. Res.* **2001**, *34*, 40. (b) Wasielewski, M. R. *Chem. Rev.* **1992**, *92*, 435. (c) Wang, M.; Wudl, F. *J. Mater. Chem.* **2012**, *22*, 24297.
- (5) Dimitrov, S. D.; Wheeler, S.; Niedzialek, D.; Schroeder, B. C.; Utzat, H.; Frost, J. M.; Yao, J.; Gillett, A.; Tuladhar, P. S.; McCulloch, I.; Nelsen, J.; Durrant, J. R. *Nat. Commun.* **2015**, *6*, 6501.
- (6) Yamamoto, Y.; Fukushima, T.; Suna, Y.; Ishii, N.; Saeki, A.; Seki, S.; Tagawa, S.; Taniguchi, M.; Kawai, T.; Aida, T. *Science* **2006**, *314*, 1761.
- (7) Dössel, L. F.; Kamm, V.; Howard, I. A.; Laquai, F.; Pisula, W.; Feng, X.; Li, C.; Takase, M.; Kudernac, T.; De Feyter, S.; Müllen, K. *J. Am. Chem. Soc.* **2012**, *134*, 5876.
- (8) Chu, C.-C.; Raffy, G.; Ray, D.; Guerso, A. D.; Kauffmann, B.; Wantz, G.; Hirsch, L.; Bassani, D. M. *J. Am. Chem. Soc.* **2010**, *132*, 12717.
- (9) Ley, D.; Guzman, C. X.; Adolffson, K. H.; Scott, A. M.; Braunschweig, A. B. *J. Am. Chem. Soc.* **2014**, *136*, 7809.
- (10) (a) Wu, Y.-L.; Brown, K. E.; Wasielewski, M. R. *J. Am. Chem. Soc.* **2013**, *135*, 13322. (b) García-Iglesias, M.; Peuntinger, K.; Kahnt, A.; Krausmann, J.; Vázquez, P.; González-Rodríguez, D.; Guldi, D. M.; Torres, T. *J. Am. Chem. Soc.* **2013**, *135*, 19311.
- (11) (a) Hizume, Y.; Tashiro, K.; Charvet, R.; Yamamoto, Y.; Saeki, A.; Seki, S.; Aida, T. *J. Am. Chem. Soc.* **2010**, *132*, 6628.
- (12) Sforazzini, G.; Orentas, E.; Bolag, A.; Sakai, N.; Matile, S. *J. Am. Chem. Soc.* **2013**, *135*, 12082.
- (13) (a) Zhang, W.; Jin, W.; Fukushima, T.; Saeki, A.; Seki, S.; Aida, T. *Science* **2011**, *334*, 340. (b) Idé, J.; Méreau, R.; Ducasse, L.; Castet, F.; Bock, H.; Olivier, Y.; Cornil, J.; Beljonne, D.; D’Avino, G.; Roscioni, O. M.; Muccioli, L.; Zannoni, C. *J. Am. Chem. Soc.* **2014**, *136*, 2911.
- (14) Sinks, L. E.; Rybtchinski, B.; Imura, M.; Jones, B. A.; Goshe, A. J.; Zuo, X.; Tiede, D. M.; Li, X.; Wasielewski, M. R. *Chem. Mater.* **2005**, *17*, 6295.
- (15) Hartnett, P. E.; Dyar, S. M.; Margulies, E. A.; Shoer, L. E.; Cook, A. W.; Eaton, S. W.; Marks, T. J.; Wasielewski, M. R. *Chem. Sci.* **2015**, *6*, 402.
- (16) Bill, N. L.; Ishida, M.; Kawashima, Y.; Ohkubo, K.; Sung, Y. M.; Lynch, V. M.; Lim, J. M.; Kim, D.; Sessler, J. L.; Fukuzumi, S. *Chem. Sci.* **2014**, *5*, 3888.
- (17) Schenning, A. P. H. J.; v. Herrikhuyzen, J.; Jonkheijm, P.; Chen, Z.; Würthner, F.; Meijer, E. W. *J. Am. Chem. Soc.* **2002**, *124*, 10252.
- (18) Hayashi, H.; Nishihashi, W.; Umeyama, T.; Matano, Y.; Seki, S.; Shimizu, Y.; Imahori, H. *J. Am. Chem. Soc.* **2011**, *133*, 10736.
- (19) Cheriya, R. T.; Joy, J.; Alex, A. P.; Shaji, A.; Hariharan, M. *J. Phys. Chem. C* **2012**, *116*, 12489.
- (20) (a) Cheriya, R. T.; Mallia, A. R.; Hariharan, M. *Energy Environ. Sci.* **2014**, *7*, 1661.
- (21) Scott Lokey, R.; Iverson, B. L. *Nature* **1995**, *375*, 303.
- (22) Rajaram, S.; Shivanna, R.; Kandappa, S. K.; Narayan, K. S. *J. Phys. Chem. Lett.* **2012**, *3*, 2405.
- (23) Rajagopal, S. K.; Philip, A. M.; Nagarajan, K.; Hariharan, M. *Chem. Commun.* **2014**, *50*, 8644.
- (24) Observed aberration in the crystal system of NIN in the crystalline vs aggregated state could arise from the reorganization of NIN assembly in CHCl₃ to form spherical architectures.
- (25) (a) Kim, J.-K.; Lee, E.; Huang, Z.; Lee, M. *J. Am. Chem. Soc.* **2006**, *128*, 14022.
- (26) (a) Kucheryavy, P.; Li, G.; Vyas, S.; Hadad, C.; Glusac, K. D. *J. Phys. Chem. A* **2009**, *113*, 6453. (b) Hasharoni, K.; Levanon, H.; Greenfield, S. R.; Gosztola, D. J.; Svec, W. A.; Wasielewski, M. R. *J. Am. Chem. Soc.* **1996**, *118*, 10228.
- (27) Inari, T.; Yamano, M.; Hirano, A.; Sugawa, K.; Otsuki, J. *J. Phys. Chem. A* **2014**, *118*, 5178.
- (28) Dance, Z. E. X.; Mickley, S. M.; Wilson, T. M.; Ricks, A. B.; Scott, A. M.; Ratner, M. A.; Wasielewski, M. R. *J. Phys. Chem. A* **2008**, *112*, 4194.
- (29) Cho, D. W.; Fujitsuka, M.; Sugimoto, A.; Yoon, U. C.; Mariano, P. S.; Majima, T. *J. Phys. Chem. B* **2006**, *110*, 11062.
- (30) Vogt, R. A.; Reichardt, C.; Crespo-Hernández, C. E. *J. Phys. Chem. A* **2013**, *117*, 6580.
- (31) Kawai, K.; Hayashi, M.; Majima, T. *J. Am. Chem. Soc.* **2012**, *134*, 4806.
- (32) Kotani, H.; Ohkubo, K.; Fukuzumi, S. *Faraday Discuss.* **2012**, *155*, 89.
- (33) Lifetime of N₂⁺ could not be measured due to the lack of NIR detector coupled to our nTA spectrometer.
- (34) Cai, X.; Tojo, S.; Fujitsuka, M.; Majima, T. *J. Phys. Chem. A* **2006**, *110*, 9319.
- (35) Gunderson, V. L.; Smeigh, A. L.; Kim, C. H.; Co, D. T.; Wasielewski, M. R. *J. Am. Chem. Soc.* **2012**, *134*, 4363.
- (36) Guzman, C. X.; Calderon, R. M. K.; Li, Z.; Yamazaki, S.; Peurifoy, S. R.; Guo, C.; Davidowski, S. K.; Mazza, M. M. A.; Han, X.; Holland, G.; Scott, A. M.; Braunschweig, A. B. *J. Phys. Chem. C* **2015**, *119*, 19584.